European Radiology (2019) 29:1787–1798
https://doi.org/10.1007/s00330-018-5720-8

BREAST

What is the diagnostic performance of 18-FDG-PET/MR compared to PET/CT for the N- and M- staging of breast cancer?

Diomidis Botsikas[1] · Ilias Bagetakos[1] · Marlise Picarra[1,2] · Ana Carolina Da Cunha Afonso Barisits[1] · Sana Boudabbous[1] · Xavier Montet[1] · Giang Thanh Lam[3] · Ismini Mainta[4] · Anastasia Kalovidouri[1] · Minerva Becker[1]

Received: 21 March 2018 / Revised: 13 July 2018 / Accepted: 14 August 2018 / Published online: 28 September 2018

Abstract

Purpose To compare the diagnostic performance of 18-FDG-PET/MR and PET/CT for the N- and M- staging of breast cancer.

Methods and materials Two independent readers blinded to clinical/follow-up data reviewed PET/MR and PET/CT examinations performed for initial or recurrent breast cancer staging in 80 consecutive patients (mean age = 48 ± 12.9 years). The diagnostic confidence for lesions in the contralateral breast, axillary/internal mammary nodes, bones and other distant sites were recorded. Sensitivity, specificity, positive (PPV) and negative predictive values (NPV) were calculated. The standard of reference included pathology and/or follow-up > 12 months.

Results Nine of 80 patients had bone metastases; 13/80 had other distant metastases, 44/80 had axillary, 9/80 had internal mammary and 3/80 had contralateral breast tumours. Inter-reader agreement for lesions was excellent (weighted kappa = 0.833 for PET/CT and 0.823 for PET/MR) with similar reader confidence for the two tests (ICC = 0.875). In the patient-per-patient analysis, sensitivity and specificity of PET/MRI and PET/CT were similar ($p > 0.05$). In the lesion-per-lesion analysis, the sensitivity of PET/MR and PET/CT for bone metastases, other metastases, axillary and internal mammary nodes, contralateral tumours and all lesions together was 0.924 and 0.6923 ($p = 0.0034$), 0.923 and 0.923 ($p = 1$), 0.854 and 0.812 ($p = 0.157$), 0.9 and 0.9 ($p = 1$), 1 and 0.25 ($p = 0.083$), and 0.89 and 0.77 ($p = 0.0013$) respectively. The corresponding specificity was 0.953 and 1 ($p = 0.0081$), 1 and 1 ($p = 1$), 0.893 and 0.92 ($p = 0.257$), 1 and 1 ($p = 1$), 0.987 and 0.99 ($p = 1$) and 0.96 and 0.98 ($p = 0.0075$) respectively.

Conclusions Reader confidence, inter-reader agreement and diagnostic performance per patient were similar with PET/MR and PET/CT. However, for all lesions together, PET/MR had a superior sensitivity and lower specificity in the lesion-per-lesion analysis.

Key Points

- *N and M breast cancer staging performance of PET/MR and PET/CT is similar per patient.*
- *In a lesion-per-lesion analysis PET/MR is more sensitive than PET/CT especially for bone metastasis.*
- *Readers' diagnostic confidence is similar for both tests.*

Keywords Positron emission tomography computed tomography · Magnetic resonance imaging · Neoplasm staging · Breast neoplasms

✉ Diomidis Botsikas
Diomidis.Botsikas@hcuge.ch

[1] Geneva University Hospital, Radiology Department, Rue Gabrielle-Perret-Gentil 4, 1205 Geneva, Switzerland

[2] Centre Hospitallier Universitaire Vaudois, Radiology Department, Rue du Bugnon 46, 1011 Lausanne, Switzerland

[3] Geneva University Hospital, Gynecology Department, Boulevard de la Cluse 30, 1211 Geneva, Switzerland

[4] Geneva University Hospital, Nuclear Medicine Department, Rue Gabrielle-Perret-Gentil 4, 1205 Geneva, Switzerland

Abbreviations

18-FDG	2-deoxy-2-(18F) fluoro-D-glucose
MIP	Maximum intensity projection
NAC	Neo-adjuvant chemotherapy
NPV	Negative predictive value
PET/CT	Positron emission tomography/computed tomography
PET/MR	Positron emission tomography/magnetic resonance
PPV	Positive predictive value

Introduction

Breast cancer is the most frequent cancer in women worldwide. It is responsible for 571,000 deaths worldwide annually [1]. Initial staging is very important for treatment planning, and survival rates depend on it. Important points for initial staging are detection of disease in the contralateral breast, evaluation of lymph node status and detection of distant metastases.

Breast magnetic resonance imaging (MRI) is the diagnostic modality with the highest sensitivity for the detection of invasive breast cancer [2, 3]. The indications when to perform pre-operative breast MRI are highly debated. Pre-operative breast MRI is in general recommended in patients with suspected multifocal, multicentric or bilateral disease (mainly newly diagnosed lobular invasive breast cancer), in newly diagnosed breast cancer in high-risk patients, in patients with major discordance between mammography and ultrasound, in younger patients, prior to partial breast irradiation but also in aggressive tumours in young patients with dense breasts [4, 5]. The technical evolution of breast MRI with more robust sequences has resulted in improved diagnostic information not only in the breast but also in the regional lymph nodes [6, 7].

The presence of distant metastases at initial presentation influences treatment options. The most frequent locations of metastatic dissemination include the lungs, liver and bony structures [8]. Whole-body 18-FDG-PET/CT (PET/CT) is a hybrid imaging modality that is useful for the initial staging of advanced breast cancer or when distant metastases are suspected [9]. It can potentially replace bone scintigraphy and when combined with diagnostic abdominal CT or MRI it can be used as the imaging modality of choice for these patients. Whole-body MRI has also been employed for the initial staging of breast cancer [10]. Regarding bone metastases, its performance is comparable to that of bone scintigraphy [11].

Whole-body and breast 18-FDG-PET/MR (PET/MR) is another, relatively recent, hybrid imaging modality that has been proposed not only for the initial staging of breast cancer [12–17] but also for the detection of recurrent disease [18]. It combines dedicated breast MRI, whole-body MRI and 18-FDG-PET.

The purpose of the current study was to compare the diagnostic performance of 18-FDG-PET/MR and PET/CT for the initial staging of breast cancer.

Methods

Patient population

This prospective study was approved by the institutional review board and written informed consent was obtained from all patients. Inclusion criteria were newly diagnosed or recurrent breast cancer with clinical indication for distal staging with PET/CT and local staging with MRI according to the pre-therapeutic multidisciplinary tumour board of our breast centre. Exclusion criteria were MRI general contraindications, pregnancy and impossibility to perform a diagnostic quality PET/MR and PET/CT examination for technical reasons. All patients included in the study underwent both whole-body 18-FDG-PET/MR and thoracic and upper-abdominal 18-FDG-PET/CT the same day between August 2010 and July 2016. The reason for this double examination was that according to our clinical experience, thin-slice high-resolution CT enables the detection of smaller pulmonary nodules than MRI. Besides, all studies that aimed to examine MRI performance for the detection of pulmonary nodules have used CT as the standard of reference [19]. Therefore, a PET/CT acquisition was obtained systematically after all PET/MR examinations performed at our institution during this period.

All examinations were retrospectively analysed from the picture archiving and communication system (PACS) of our institution and two experienced readers (7 years of experience each) performed an independent and blinded reading of all PET/MR and PET/CT examinations. All patients' clinical parameters, biopsy results, final pathology results and follow-up examinations were retrieved from the medical records of our institution. Patients with unavailable standard of reference were excluded from the study.

PET/MR acquisition

PET/MR examinations were performed on a Philips Ingenuity TF PET/MR (Philips Healthcare), which is a sequential PET/MR system with both scanners (MR and PET) located in the same room. All patients underwent a 3-T MRI acquisition and PET scanning. Transfer from the 3-T MRI scanner to the PET scanner was done by means of a rotating table allowing the patient to remain in the same position. For the MR-based attenuation correction of PET data, a correction map was calculated using three-class segmentation (air, lung and soft tissue) of a 3D multi-stack T1-weighted spoiled gradient echo sequence, with assignment of predefined attenuation coefficients to each class and addition of a previously generated

template for the table and the RF coil attenuation of the emission data. PET images were reconstructed using a three-dimensional line-of-response (LOR)/TF/blob-based ordered subset expectation maximisation (3D-OSEM) algorithm (3 iterations × 33 subsets, as recommended by the manufacturer, voxel size 4 × 4 × 4 mm).

Each patient was injected with a total of 3.5 MBq/kg of 18F-FDG, after having fasted for at least 6 h. Immediately after injection, an MR examination from the vertex to the symphysis pubis (axial T1-weighted Dixon and coronal T2-weighted single shot) was performed in the supine position to benefit from the waiting time for radiotracer distribution in the body. A whole-body PET acquisition with the same coverage was performed subsequently (10 beds, 1.5 min/bed). The patient then underwent breast MRI with a dedicated breast coil in the prone position (axial T2-weighted DWI including b0 and b1000 values and dynamic enhanced T1-weighted Dixon sequences) after iv injection of 0.2 ml/kg of gadoterate meglumine (Dotarem, Guebert) with an injection rate of 4 ml/s. Finally a dedicated breast PET (3 beds 3 min/bed) in the prone position covering the axillary regions was performed. The whole examination lasted approximately 90 min. The detailed technical protocol is shown in Table 1 and illustrated in Fig. 1.

PET/CT acquisition

PET/CT scans were performed immediately after PET/MR (average time = 185 min after tracer injection) on either a Biograph 64 scanner (44 patients) or a Biograph mCT scanner (36 patients) (Siemens Medical Solutions). A PET/CT scan covering the thoracic and upper abdominal region was acquired with 3-4 min per bed position, depending on the patient's weight for the PET and 120 kVp, 60 mAs, pitch 1.5 and 1 s per rotation for the CT scan. The CT was used for the attenuation correction of the emission data. PET images were reconstructed using a three-dimensional iterative ordered subset expectation maximisation (3D-OSEM) algorithm (4 iterations × 8 subsets) followed by a 5-mm FWHM post-processing Gaussian filter. The voxel size was 4 × 4 × 5 mm, comparable to the one obtained by the PET/MR system.

PET/MR and PET/CT interpretation

All images were anonymised and transferred to dedicated workstations (OsiriX, Pixmeo). They were interpreted by two independent readers with 7 years of experience in PET/CT and 6 years in MRI, respectively. One of the readers was a member of the women's imaging division and the other of the musculoskeletal imaging division of the imaging department of our hospital with respective experience in breast and musculoskeletal MRI. Both readers underwent a training session for the interpretation of whole-body and breast MR and PET/MR under the supervision of the referral radiologists for women and skeletal imaging in our institution, both of whom had at least 15 years of MRI and PET/CT experience in their respective field of expertise. In this training session they evaluated in

Table 1 Detailed PET/MR acquisition protocol

PET/MR technical protocol			
Whole-body protocol (supine)	Time (min)	Resolution (mm)	TR/TE (ms)
Calibration, survey and reference scan	05:00	-	-
T2 TSE coronal *	05:00	1.47/1.46/8.00	3280/76
DWIBS axial (single-shot EPI)	10:30	1.46/1.45/7.00	3929/49 (TI = 230)
3D T1 mDixon WB axial*	02:17	0.85/0.85/3.00	3.2/1.11/2.0
atMR (3D T1 FFE)	03:00	1.88/1.88/6.00	4.1/2.3
PET WB (10 beds × 1.5 min)	15:00	4.00/4.00/4.00	-
	40:47		
Breast protocol (prone)	Time (min)	Resolution (mm)	TR/TE (ms)
Calibration, survey and reference scan	03:00	-	-
T2 TSE axial	03:20	0.59/0.59/3.00	5000/120
DWI b0/b1000 (single-shot EPI)	02:32	1.18/1.18/3.00	10,101/69
3D T1 Dixon axial unenhanced	01:28	0.60/0.60/1.30	7.8/2.4/5.4
3D T1 Dixon axial dynamic enhanced (6 frames)**	08:48	0.60/0.60/1.30	7.8/2.4/5.4
atMR breast (3D T1 FFE)	01:06	1.88/1.88/6.00	4.1/2.3
PET breast (3 beds × 3 min)	09:00	4.00/4.00/4.00	-
	29:14		

*Breathold sequences

**First dynamic series 90 s after Gd injection

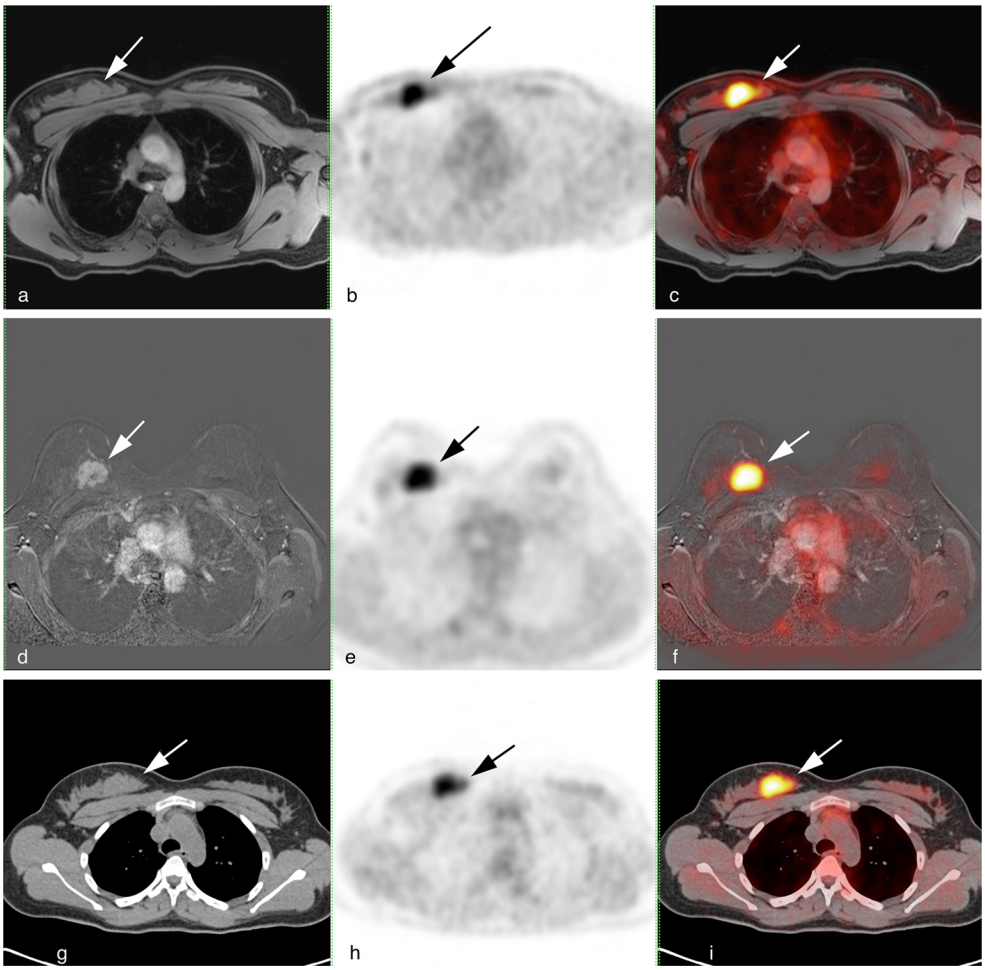

Fig. 1 A 38-year-old patient with grade 3 invasive ductal carcinoma of the right breast pT2, pN2, M0. Illustration of the acquisition protocol of PET/MR and PET/CT examinations. Whole-body Dixon T1W MRI (**a**) with corresponding PET (**b**) and fusion PET/MR images (**c**) in the supine position, followed by dedicated breast MRI (**d**) with corresponding PET (**e**) acquisition and fused PET/MR (**f**) in the prone position and late PET/CT (**g**, **h**, **i**) supine acquisitions. Notice the mass lesion of the inner upper quadrant (arrows in all images). The lesion is detected on enhanced breast MRI (**d**) because of its contrast uptake. It is also clearly visible on PET in all three acquisitions (**b**, **e**, **h**) because of its intense metabolism. However, as expected, it is almost invisible on both unenhanced T1W MR (**a**) and unenhanced CT (**g**)

consensus the PET/MR examinations of the five patients that were excluded from the study because of unavailability of the standard of reference. Then, the two readers evaluated the PET/MR and PET/CT examinations separately with a delay of at least 3 months between the two readings for the same patient. They were blinded to the final diagnosis and to the second reader's interpretation. However, they had access to the clinical indication and patients' history as known up to the date of the examination, thus simulating real clinical conditions. Real clinical conditions were simulated for PET/CT and PET/MR respectively and the readers were able to perform reconstructions in different planes, freely change window settings for all CT, MRI and PET image series and fusion of the appropriate PET series with the corresponding CT and MR series at their convenience and in the desired plane. Maximum intensity 3D projections (MIP) were also performed according to reader's preferences.

Each reader noted in each patient all suspicious lesions found in the contralateral breast of the known cancer, all axillary, internal mammary, mediastinal and other lymph node localisations, bone lesions, pulmonary and other distant metastases, and their size and exact localisation. Up to five lesions per patient per organ were registered. Lymph node assessment was done per group, as—based on the surgical specimen available—it was not possible to precisely correlate lymph nodes detected by imaging with surgically harvested lymph nodes within a group. Therefore, if a lymph node was considered positive at imaging, the whole group was labelled as positive and, vice versa, if a single lymph node was positive at histopathology, the whole group was considered positive.

The criteria for PET/MR image interpretation and for PET/CT interpretation were based on the recommendations in the literature [14, 15, 20] combining the diagnostic criteria of MRI and PET and CT and PET according to the readers' clinical judgement. For all lesions, the diagnostic confidence was noted using a scale from 1 to 4 (1 = probably not a malignant lesion, 2 = possibly not malignant, 3 = possibly malignant and 4 = most probably a malignant lesion). For a lesion with a diagnostic score of 1 and 2, the examination was considered negative for malignancy. For lesions with a diagnostic score of 3 and 4, the examination was considered positive for malignancy. When there was discrepancy between the two readers, a consensus reading session with both readers and an additional third reader with 12 years' experience in female imaging was organised. In the results section of this article the diagnostic performance of this consensus reading will be presented.

According to the readers' findings, N and M staging according to PET/MR and PET/CT was performed and compared with the standard of reference.

Standard of reference

When available, percutaneous biopsy and final pathological analysis were used as the standard of reference. For cases without pathology results a follow-up of at least 1 year (mean 819 days, range 370-2342) was used as the standard of reference. For all patients with loco-regional lesions proven at histopathology, follow-up was used for eventual metastatic lesions. Only patients with absence of metastatic lesions during at least 1-year follow-up were considered negative for metastatic lesions. Patients who underwent neo-adjuvant chemotherapy (NAC) and had no residual lesion at final pathology results were excluded from the study if no prior percutaneous biopsy had been performed. Patients with less than 12 months of follow-up and no pathology results were also excluded from the study. Lesions that were positive for malignancy before NAC proven by percutaneous biopsy were considered positive, independently of the final pathological report after NAC. Suspicious lesions that decreased in size together with the primary tumour after NAC were considered positive for malignancy.

Concerning the type of follow-up, all patients without evidence of metastatic disease at presentation had a mammography, breast and axillary ultrasound and clinical examination annually after surgery and no further total body radiological examination was performed if there was not a clinical or radiological suspicion of recurrent loco-regional or metastatic disease ($n = 66$). Additionally to this annual standard follow-up, seven patients had CT, two had PET-CT, two had PET/CT and MRI and three MRI only.

For all comparisons, only lesions located in the thoracic and upper abdomen as covered by the PET/CT were analysed. Any lesions detected at PET/MR that were outside the field of view of PET/CT were not included in the analysis.

Statistical analysis

Inter-reader agreement was tested with the calculation of the kappa correlation coefficient for both PET/CT and PET/MR. Diagnostic confidence for both examinations was tested by calculation of the intra-class correlation coefficient based on the readers' score of 1-4. Sensitivity, specificity, positive (PPV) and negative predictive values (NPV) were calculated for both PET/MR and PET/CT examinations on a lesion-per-lesion and patient-per-patient basis and were compared with McNemar's test. Comparison between N and M staging as determined by PET/MR and PET/CT versus the standard of reference was performed with calculation of Cohen's kappa coefficient.

Statistical analyses were performed with Prism® 6 for Mac OS X, v6.0d Graphpad Software Inc. and R software (R.app GUI 1.53 S. Urbanek & H.-J. Bibiko, © R Foundation for Statistical Computing, 2012).

Results

From the 85 patients that underwent PET/MR and PET/CT, 5 were excluded because the standard of reference was not available (no follow-up in 3 and no residual disease after NAC in 2 patients without initial percutaneous biopsy results). The remaining 80 patients (mean age = 48 ± 12.9 years) formed the population of our study. The standard of reference consisted of final pathology results in 33 patients, percutaneous biopsy results in 31 patients and radiological and clinical follow-up of more than 12 months in the remaining 16 patients. On a per-lesion basis, 9 bone metastases were confirmed with percutaneous biopsy and 48 axillary lymph node localisations were confirmed by pathology of the surgical specimen with or without percutaneous biopsy before surgery. Four contralateral breast tumours were confirmed by percutaneous biopsy and final pathology results. Additionally, from the other distant metastatic lesions, one of multiple liver metastases and one of multiple pulmonary metastases as well as one pleural and one thoracic wall lesion were confirmed by percutaneous biopsies. Seventeen bone lesions, 10 internal mammary lymph nodes, 6 mediastinal lymph nodes, 2 infraclavicular lymph nodes and 1 thoracic wall lesion were confirmed on follow-up. Percutaneous biopsies were performed on average 8 days before and 101 days after PET/MR and PET/CT, while surgery followed on average 52 (range 3-166) days after imaging evaluation. The reason for this wide range is that in many cases, for example for loco-regional lymph nodes, the percutaneous biopsy was performed before PET/MR, at the same time as the initial tumour detection on the basis of conventional imaging, while other biopsies were performed after imaging and even after treatment, as for example for tumours that were initially considered benign but were found to progress during the follow-up and also for lesions for which biopsy was decided after the end of neoadjuvant chemotherapy (NAC).

At presentation, 15 patients had clinical stage I disease, 39 stage II, 13 stage III and 11 stage IV. One patient had axillary lymph node recurrence and one had primary breast angiosarcoma. Table 2 shows detailed patient and tumour characteristics.

Based on the standard of reference, a total of 101 metastatic lesions were present in 51/80 patients; 9 patients had 26 bone metastases (mean diameter = 2.2 ± 1.4 cm), 8 had other distant metastases (1 patient with multiple hepatic metastases, 2 with mediastinal and infra-clavicular lymph node metastases, 1 with pleural, thoracic wall and mediastinal lymph nodes, 3

Table 2 Detailed patient and tumour characteristics

Patient population		
Age years +/- StdD	48 ± 12.9	
BMI ± SD	24 ± 4.02	
	Number	Percentage %
Number of patients	80	100
Females	80	100
Tumour histology		
Invasive ductal carcinoma	69	86.25
Invasive lobular carcinoma	5	6.25
Other histologies	6	7.5
Histological grade		
I	3	4.05
II	41	55.41
III	30	40.54
ER status		
Positive	49	64.47
Negative	27	35.53
PR status		
Positive	44	57.89
Negative	32	42.11
Ki67 index status		
< 20%	13	17.11
≥ 20%	63	82.89
HER2 status		
Positive	33	43.42
Negative	43	56.58
Breast cancer subtype		
Luminal	52	68.42
HER positive	12	15.79
Triple negative	12	15.79

ER oestrogen receptor, *PR* progesterone receptor, *HER2* human epidermal growth factor receptor 2

with mediastinal metastases only and one with multiple pulmonary and mediastinal metastases); 46 patients had 48 axillary metastases (44 homolateral and 2 bilateral; mean small diameter = 1.2 ± 1 cm), 9 had internal mammary metastases (8 homolateral and 1 bilateral; mean small diameter = 0.6 ± 0.1 cm) and 3 patients had 4 contralateral breast tumours (mean size = 0.9 ± 0.5 cm). One of the patients with multiple bone metastases also had three pelvic bone lesions seen on PET/MR. As these lesions had not been covered in the field of view of PET/CT they were excluded from the per-lesion analysis.

Thirteen patients had metastatic M1 disease, including bone, liver, pulmonary, mediastinal, pleural and thoracic wall metastases.

Inter-reader agreement for lesion detection was excellent (weighted kappa = 0.833 for PET/CT and 0.823 for PET/MR). Diagnostic confidence of both readers between the two tests was similar (ICC = 0.875).

Sensitivity, specificity PPV and NPV in the lesion-per-lesion analysis and for all lesions together with PET/MR and PET/CT were 0.89, 0.96, 0.82, 0.98 and 0.77, 0.98, 0.89, 0.96 respectively. PET/MR had a significantly higher sensitivity (p = 0.0013) while PET/CT a slightly higher but statistically significant specificity (p = 0.0075). Detailed results of the lesion-per-lesion analysis are shown in Table 3. As shown in this table, especially for bone lesions, PET/MR was more sensitive and PET/CT was more specific, while for axillary and internal mammary lymph nodes there was no significant difference for the diagnostic performance of the two tests. Figure 2 shows a patient with multiple lymph node and bone metastases, detected on both modalities.

The eight false-negative bone lesions for PET/CT had a mean size of 1.5 ± 0.3 cm while the two false-negative bone lesions for PET/MR measured 1.3 cm and 1.6 cm respectively. The main reason for not detecting lesions on PET/CT was their very low conspicuity on CT compared with MRI and the low FDG uptake (Fig. 3). Concerning contralateral breast lesions and distant metastases, including mediastinal lymph nodes, liver, pulmonary, pleural and thoracic wall lesions, the number of lesions was too small to extract statistically relevant results.

Despite a trend for higher sensitivity for PET/MR and higher specificity for PET/CT in the lesion-per-lesion analysis, no statistically significant difference between the diagnostic performances of the two tests was found in the patient-per-patient analysis as shown in Table 4.

Cohen's kappa correlation coefficient for PET/MR N staging versus standard of reference N staging was 0.484 and for PET/CT N staging versus standard of reference N staging was 0.536. For PET/MR M staging versus standard of reference M staging, kappa was 0.817; for PET/CT M staging versus standard of reference M staging, kappa was 0.800.

Discussion

Whole-body PET/MR is a hybrid modality that has recently been proposed as an alternative to conventional radiological examinations, bone scintigraphy and PET/CT for breast cancer staging. If combined with dedicated breast PET/MR it offers a potentially attractive one-stop-shop solution for patients with advanced breast cancer who should undergo both breast MRI for local staging and whole-body PET/CT for distant staging [13].

Different authors have published their experience with breast PET/MR, some applying only a whole-body PET/MR protocol [16, 21] and others whole-body combined with dedicated breast PET/MR [14, 15, 22–24]. In our institution we preferred performing whole-body and breast PET/MR in the same examination rather than programming a separate breast MRI and whole-body PET/MR examination for the patient.

Table 3 Diagnostic performance of PET/MR and PET/CT in a per-lesion analysis showing the number of true-negative (TN), true-positive (TP), false-negative (FN) and false-positive (FP) cases as well as sensitivities (SENS), specificities (SPEC), positive and negative predictive values (PPV and NPV) for each modality, with corresponding *p* values

Per-lesion results

All lesions together				Bone metastases			Contra-lateral breast cancer			Axillary lymph nodes			Internal mammary lymph nodes			Mediastinal lymph nodes		
Prevalence metastases	101/662 (15.25%)			26/175 (14.85%)			4/82 (4.88%)			48/160 (30%)			10/160 (6.25%)			6/80 (7.5%)		
	p	PET/MR	PET/CT	*p*	PET/MR	PET/CT	*p*	PET/MR	PET/CT	*p*	PET/MR	PET/CT	*p*	PET/MR	PET/CT	*p*	PET/MR	PET/CT
TN		541	551		142	149		77	77		100	103		150	150		74	74
TP		90	78		24	18		4	1		41	39		9	9		6	6
FN		11	23		2	8		0	3		7	9		1	1		0	0
FP		20	10		7	0		1	1		12	9		0	0		0	0
SENS	0.0013	0.89 [0.81–0.94]	0.77 [0.67–0.85]	0.0034	0.92 [0.73–0.99]	0.69 [0.48–0.85]	0.083	1.00 [0.40–1]	0.25 [0.01–0.78]	0.157	0.85 [0.72–0.93]	0.81 [0.67–0.90]	N/A	0.90 [0.54–0.99]	0.90 [0.54–0.99]	N/A	1.00 [0.52–1]	1.00 [0.52–1]
SPEC	0.0075	0.96 [0.94–0.98]	0.98 [0.97–0.99]	0.0081	0.95 [0.90–0.98]	1.00 [0.97–1]	N/A	0.99 [0.92–1]	0.99 [0.92–1]	0.257	0.89 [0.82–0.94]	0.92 [0.85–0.96]	N/A	1.00 [0.97–1]	1.00 [0.97–1]	N/A	1.00 [0.94–1]	1.00 [0.94–1]
PPV		0.82 [0.73–0.88]	0.89 [0.80–0.94]		0.77 [0.58–0.90]	1.00 [0.78–1]		0.80 [0.30–0.99]	0.50 [0.03–0.97]		0.77 [0.63–0.87]	0.81 [0.67–0.91]		1.00 [0.63–1]	1.00 [0.63–1]		1.00 [0.52–1]	1.00 [0.52–1]
NPV		0.98 [0.96–0.99]	0.96 [0.94–0.97]		0.99 [0.95–1]	0.95 [0.90–0.98]		1.00 [0.94–1]	0.96 [0.89–0.99]		0.93 [0.86–0.97]	0.92 [0.85–0.96]		0.99 [0.96–1]	0.99 [0.96–1]		1.00 [0.94–1]	1.00 [0.94–1]

P values for the pairwise comparison of the sensitivity and specificity of PET/MR and PET/CT were calculated using the McNemar test. Other metastatic sites. Supraclavicular lymph nodes = 2 patients TP on both PET/MR and PET/CT, Multiple pulmonary metastases = 1 patient on both PET/MR and PET/CT, Pleural metastases = 1 patient TP on both PET/MR and PET/CT, Multiple liver metastases = 1 patient FN on both PET/MR and PET/CT, Thoracic wall metastases = 2 patients TP on both PET/MR and PET/CT

TN true negative, *TP* true positive, *FN* false negative, *FP* false positive, 95% confidence intervals are indicated in square brackets, *SENS* sensitivity, *SPEC* specificity, *PPV* positive predictive value, *NPV* negative predictive value

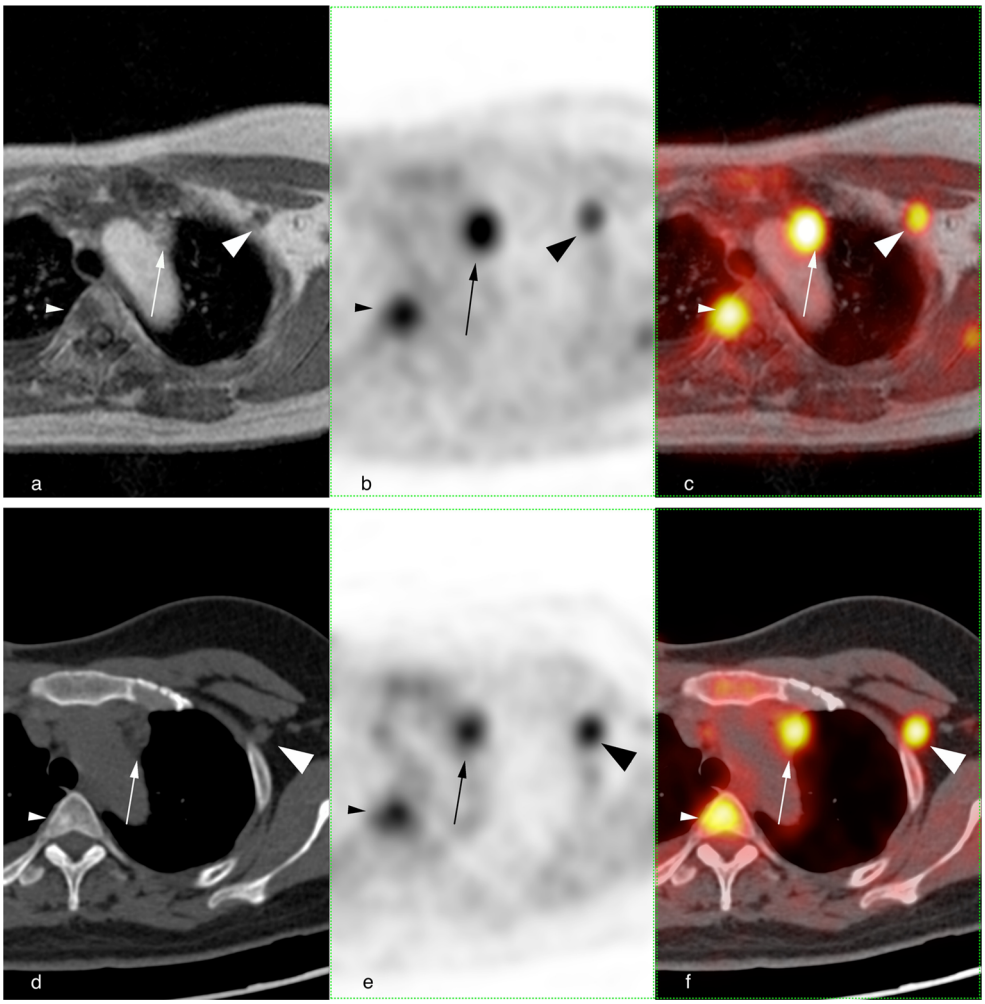

Fig. 2 PET/MR (**a**, **b**, **c**) and PET/CT (**d**, **e**, **f**) of a 37-year-old patient with grade 3 invasive ductal carcinoma of the right breast stage pT2, N3, M1. The axial plane Dixon T1W MR (**a**), corresponding PET (**b**) and fused PET/MR images (**c**) show a vertebral body metastatic lesion (small arrowhead), anterior mediastinal infiltrated lymph node (arrow) and retropectoral infiltrated lymph node (big arrowhead). The same lesions are seen on the CT (**d**), PET (**e**) and fused PET/CT (**f**) images. All lesions were unequivocally considered metastatic on both techniques by both readers (score 4)

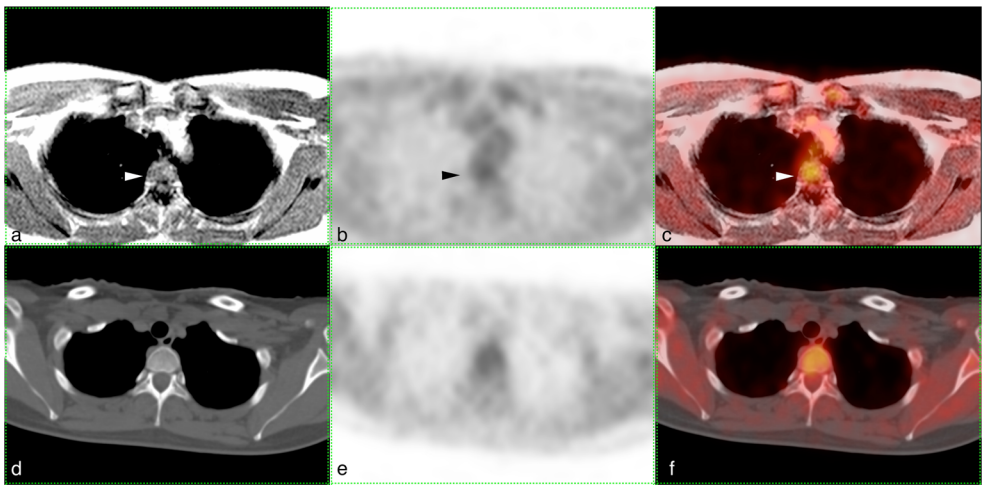

Fig. 3 PET/MR (**a**, **b**, **c**) and PET/CT (**d**, **e**, **f**) of a 41-year-old patient with grade 3 invasive ductal carcinoma of the left breast pT2, N1, M1. Axial Dixon T1W MR (**a**), PET (**b**) and fused PET/MR (**c**) show a single focal slight hypermetabolism in a thoracic vertebral body associated with a focal hypointensity in the vertebral body on MRI (arrowhead in **a**, **b**, **c**). Corresponding PET/CT images did not reveal any focal uptake or morphological pathological lesion. This case was considered positive on PET/MR with a confidence score of 3 by both readers and as negative on PET/CT

Table 4 Diagnostic performance of PET/MR and PET/CT in a per-patient analysis showing the number of true-negative (TN), true-positive (TP), false-negative (FN) and false-positive (FP) cases as well as sensitivities (SENS), specificities (SPEC), positive and negative predictive values (PPV and NPV) for each modality, with corresponding *p* values

Per-patient results																	
All metastases together *(M1)				Bone metastases			Contralateral breast tumours			Axillary lymph nodes			Internal mammary lymph nodes			Mediastinal lymph nodes		
Prevalence metastases	13/80 (16.25%)			9/80 (11.25%)			3/80 (3.75%)			46/80 (57.5%)			9/80 (11.25%)			6/80 (7.5%)		
	p	PET/MR	PET/CT	*p*	PET/MR	PET/CT	*p*	PET/MR	PET/CT	*p*	PET/MR	PET/CT	*p*	PET/MR	PET/CT	*p*	PET/MR	PET/CT
TN		65	67		69	71		76	76		23	26		71	71		74	74
TP		11	9		8	6		3	1		40	38		8	8		6	6
FN		2	4		1	3		0	2		6	8		1	1		0	0
FP		2	0		2	0		1	1		11	8		0	0		0	0
SENS	0.157	0.85 [0.54–0.97]	0.69 [0.39–0.90]	0.157	0.89 [0.51–0.99]	0.67 [0.31–0.91]	0.157	1.00 [0.31–1]	0.33 [0.02–0.87]	0.157	0.87 [0.73–0.95]	0.83 [0.68–0.91]	N/A	0.89 [0.51–0.99]	0.89 [0.51–0.99]	N/A	1.00 [0.52–1]	1.00 [0.52–1]
SPEC	0.157	0.97 [0.89–0.99]	1.00 [0.93–1]	0.157	0.97 [0.89–0.99]	1.00 [0.94–1]	N/A	0.99 [0.92–1]	0.99 [0.92–1]	0.18	0.68 [0.49–0.82]	0.76 [0.58–0.89]	N/A	1.00 [0.94–1]	1.00 [0.94–1]	N/A	1.00 [0.94–1]	1.00 [0.94–1]
PPV		0.85 [0.54–0.97]	1.00 [0.63–1]		0.80 [0.44–0.96]	1.00 [0.52–1]		0.75 [0.22–0.99]	0.50 [0.03–0.97]		0.78 [0.64–0.88]	0.83 [0.68–0.92]		1.00 [0.60–1]	1.00 [0.60–1]		1.00 [0.52–1]	1.00 [0.52–1]
NPV		0.97 [0.89–0.99]	0.94 [0.85–0.98]		0.99 [0.91–1]	0.96 [0.88–0.99]		1.00 [0.94–1]	0.97 [0.90–0.99]		0.79 [0.60–0.91]	0.76 [0.58–0.89]		0.99 [0.91–1]	0.99 [0.91–1]		1.00 [0.94–1]	1.00 [0.94–1]

TN true negative, *TP* true positive, *FN* false negative, *FP* false positive, 95% confidence intervals are indicated in square brackets, *SENS* sensitivity, *SPEC* specificity, *PPV* positive predictive value, *NPV* negative predictive value. *P* values for the pairwise comparison of the sensitivity and specificity of PET/MR and PET/CT were calculated using the McNemar test

*Patients with bone, liver, pulmonary, mediastinal, pleural, thoracic wall metastases

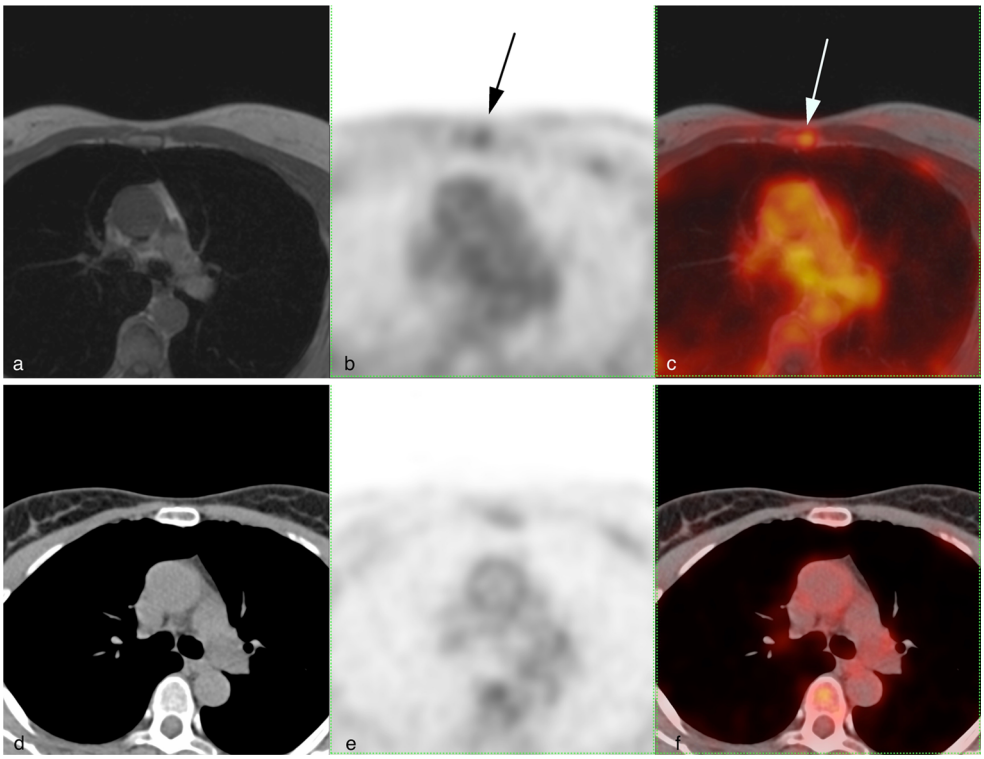

Fig. 4 PET/MR (**a**, **b**, **c**) and PET/CT (**d**, **e**, **f**) of a 60-year-old patient with grade 3 invasive lobular carcinoma of the right breast pT3, pN2a, M1. Arrows on axial PET (**b**) and fused PET/MR (**c**) show a single focal slight hypermetabolism in the sternum. Corresponding PET/CT images did not reveal any focal uptake or morphological pathological lesion. Despite no lesion being visible on the corresponding Dixon T1W MR (**a**) images, this case was considered positive on PET/MR with a confidence score of 3 by both readers and negative on PET/CT. On the last thoracic CT scan 2 years after the initial investigations there was no visible sternal lesion, while the patient died 3 months later with multiple other bone and brain metastases. It was a false positive of PET/MR and true negative of PET/CT

In our study, we compared unenhanced whole-body PET/MR and PET/CT. In the patient-per-patient analysis we found no statistically significant difference in sensitivity, specificity, PPV and NPV of the two tests, while in the lesion-per-lesion analysis, PET/MR had a significantly higher sensitivity for bone metastases but similar sensitivity to PET/CT for axillary and internal mammary lymph nodes. The reason for this difference isthat T1-weighted MRI sequences reveal metastatic bone lesions by showing bone marrow replacement. Thus, a faint radiotracer uptake on PET, if combined with an MRI-positive finding, results in a positive PET/MR finding. On the contrary, a faint uptake on PET that is not associated with a corresponding CT finding results in a negative PET/CT evaluation. So, the main reason for not detecting lesions on PET/CT was their very low conspicuity on CT compared with MRI. This mechanism could be the reason for the better sensitivity of PET/MR. Other metastatic localisations were too few in this study to allow reliable conclusions. Corresponding specificities were slightly but significantly higher for PET/CT. This might be explained by the fact that PET/CT acquisition was performed later than PET/MR. As reported in the literature, contrast between tumour and background (bone marrow, breast parenchyma, mediastinum, myocardium, and liver) but also between tumour and benign lesions [25, 26] is significantly higher in late 3 h acquisitions compared with early 1.5 h. Figure 4 shows a false-negative bone lesion seen only in PET/MR.

Comparison between whole-body PET/MR and PET/CT for breast cancer patients has been the subject of different studies. However, as the protocols of the corresponding examinations were not homogeneous, it is difficult to compare these studies with our results. Jeong et al [22] studied the anatomic correlation of PET/MR with a whole-body Dixon T1-weighted sequence compared with that of enhanced PET/CT and found that the score of enhanced PET/CT was significantly better. In our study we used the same Dixon T1-weighted MR sequence for whole-body PET/MR attenuation correction. However, unlike Jeong et al, we aimed to direct comparison of diagnostic performances of the two tests. Moreover, in our study, both PET/MR and PET/CT were unenhanced.

In another study, Pace et al [21] did not find any significant difference for the detection of metastatic lesions between unenhanced PET/CT and PET/MR in a small series of 36 patients.

Melsaether et al [16] compared the sensitivity of contrast enhanced PET/MR with that of unenhanced PET/CT in a series of 51 patients with breast cancer. They found that PET/MR and PET/CT had similar sensitivities for metastatic disease in the patient-per-patient analysis but PET/MR outperformed PET/CT for bone and liver metastases in the lesion-per-lesion analysis. However, this study did not evaluate the specificities of the two tests.

Catalano et al [14] evaluated the diagnostic performance of contrast-enhanced PET/MR and PET/CT for bone metastases in a series of 109 breast cancer patients and found that contrast-enhanced PET/MR had a significantly higher sensitivity than contrast-enhanced PET/CT on a patient-per-patient basis.

In this study we performed unenhanced whole-body MRI as we reserved the iv gadolinium injection for the dedicated breast MRI in the prone position. This might have negatively influenced the diagnostic performance of PET/MR for distant lesions. Concerning contralateral breast lesions, dedicated PET/MR largely outperformed PET/CT (detection of 4 out of 4 lesions versus 1 out of 4 for PET/CT), but this was mainly due to the contribution of the dedicated breast MR.

Concerning N and M staging estimated by PET/MR and PET/CT versus the standard of reference, kappa values for both tests were similar. Especially for N staging, Cohen's kappa correlation coefficient for PET/MR versus standard of reference N staging was 0.484 and for PET/CT versus standard of reference N staging was 0.536. These kappa values for N staging are relatively low. This can be explained by the fact that we chose not to report a weighted kappa coefficient (N+ versus N-) but rather to correlate the exact N staging. As N staging depends on the number of infiltrated LNs, the differences between radiological N staging and pathological N staging can probably be explained by the fact that the number of infiltrated LNs reported on PET/MR and PET/CT was different from that found on pathology, which included small metastatic deposits not always visible on imaging.

In a similar approach, Catalano et al [27] found that whole-body PET/MR was more accurate in correctly predicting the initial stage of breast cancer than whole-body DWI MRI, but the discrepancies were not statistically significant ($p = 0.14$). Another study [28] evaluated the diagnostic performance of PET/MR for axillary nodal staging and found that PET/MR changed the staging in 22% of patients compared with PET/CT. However, these results are based on a population of nine patients and no safe conclusions can be drawn.

Sawicki et al reported the results of comparison of PET/MR, PET/CT, CT and MRI in recurrent breast cancer patients [20]. According to their study, PET/MR had a higher sensitivity and specificity compared with PET/CT on a lesion-per-lesion basis but not on a patient-per-patient analysis. However, this study included a very important number of malignant lesions and 17 of 21 patients included had recurrent disease. In this context of very high suspicion of metastatic disease, PET/MR can be a valuable tool for staging.

Our study has limitations. First of all, PET/CT was performed with an important time delay after injection of radiotracer compared with PET/MR. This was inevitable as the patient had to finish the first examination and then be transferred to the PET/CT for the acquisition of PET/CT images. However, according to the literature [25, 26] delayed 3-h post-injection acquisitions are more sensitive for detection of breast cancer lesions. Thus, the difference between the performances of the two techniques due to the delay of PET/CT compared with PET/MR would have been important if PET/CT was found to be more sensitive than PET/MR, which was not the case in our study. On the contrary, PET/MR, despite an earlier acquisition after radiotracer injection, was still found to be more sensitive. Another relative limitation of the study was that the coverage of both tests was not the same. However, to compensate for the different fields of view with both examinations, we analysed only the areas that had identical coverage on PET/MR and PET/CT, respectively. For this reason, three pelvic bone metastatic lesions were excluded because they were seen only in PET/MR but not on PET/CT because of the non-coverage of the pelvis on this latter modality.

In conclusion, PET/MR was associated with a higher sensitivity than PET/CT for metastatic lesions, mainly because of its performance for bone and breast lesions. However, there was no statistically significant difference in the patient-per-patient analysis, as well as for N and M staging. Further prospective studies with larger populations are needed to confirm whether PET/MR outperforms PET/CT for the detection of breast cancer metastases on a patient-per-patient basis.

Funding The authors state that this work has not received any funding.

Compliance with ethical standards

Guarantor The scientific guarantor of this publication is Diomidis Botsikas. MD, Privat Docent (PD).

Conflict of interest All authors declare no conflict of interest.

Statistics and biometry One of the authors has significant statistical expertise.

No complex statistical methods were necessary for this article.

Informed consent Written informed consent was obtained from all subjects (patients) in this study.

Ethical approval Institutional Review Board approval was obtained.

Study subjects or cohorts overlap Data of PET/MR examinations of 42 patients were included in the article below. This article focused on the diagnostic performance of PET/MR in loco-regional staging of breast cancer and data of PET/CT were not analysed. This same article also included PET/MR after neoadjuvant systemic treatment while the present manuscript includes only data from the initial PET/MR study.

Clinical utility of 18F-FDG-PET/MR for preoperative breast cancer staging. Botsikas D, Kalovidouri A, Becker M, Copercini M, Djema DA, Bodmer A, Monnier S, Becker CD, Montet X, Delattre BM, Ratib O, Garibotto V, Tabouret-Viaud C. Eur Radiol. 2016 Jul;26(7):2297-307. doi: 10.1007/s00330-015-4054-z. Epub 2015 Oct 17.

Methodology
- prospective
- diagnostic or prognostic study
- performed at one institution

References

1. Organisation WH (2017) Cancer Fact Sheet. In: World Health Organisation. Available via http://www.who.int/news-room/fact-sheets/detail/cancer.
2. Houssami N, Ciatto S, Macaskill P et al (2008) Accuracy and surgical impact of magnetic resonance imaging in breast cancer staging: systematic review and meta-analysis in detection of multifocal and multicentric cancer. J Clin Oncol 26:3248–3258
3. Mariscotti G, Houssami N, Durando M et al (2014) Accuracy of mammography, digital breast tomosynthesis, ultrasound and MR imaging in preoperative assessment of breast cancer. Anticancer Res 34:1219–1225
4. Sardanelli F, Boetes C, Borisch B et al (2010) Magnetic resonance imaging of the breast: recommendations from the EUSOMA working group. Eur J Cancer 46:1296–1316
5. Mann RM, Kuhl CK, Kinkel K, Boetes C (2008) Breast MRI: guidelines from the European Society of Breast Imaging. Eur Radiol 18:1307–1318
6. Dietzel M, Baltzer PA, Vag T et al (2010) Application of breast MRI for prediction of lymph node metastases—systematic approach using 17 individual descriptors and a dedicated decision tree. Acta Radiol 51:885–894
7. Baltzer PA, Dietzel M, Burmeister HP et al (2011) Application of MR mammography beyond local staging: is there a potential to accurately assess axillary lymph nodes? evaluation of an extended protocol in an initial prospective study. AJR Am J Roentgenol 196: W641–W647
8. Weigelt B, Peterse JL, van 't Veer LJ (2005) Breast cancer metastasis: markers and models. Nat Rev Cancer 5:591–602
9. Gradishar WJ, Anderson BO, Blair SL et al (2014) Breast cancer version 3.2014. J Natl Compr Canc Netw 12:542–590
10. Lauenstein TC, Freudenberg LS, Goehde SC et al (2002) Whole-body MRI using a rolling table platform for the detection of bone metastases. Eur Radiol 12:2091–2099
11. Gutzeit A, Doert A, Froehlich JM et al (2010) Comparison of diffusion-weighted whole body MRI and skeletal scintigraphy for the detection of bone metastases in patients with prostate or breast carcinoma. Skeletal Radiol 39:333–343
12. Taneja S, Jena A, Goel R, Sarin R, Kaul S (2014) Simultaneous whole-body ^{18}3F-FDG PET-MRI in primary staging of breast cancer: a pilot study. Eur J Radiol 83:2231–2239
13. Tabouret-Viaud C, Botsikas D, Delattre BM et al (2015) PET/MR in Breast Cancer. Semin Nucl Med 45:304–321
14. Catalano OA, Nicolai E, Rosen BR et al (2015) Comparison of CE-FDG-PET/CT with CE-FDG-PET/MR in the evaluation of osseous metastases in breast cancer patients. Br J Cancer 112:1452–1460
15. Botsikas D, Kalovidouri A, Becker M et al (2016) Clinical utility of 18F-FDG-PET/MR for preoperative breast cancer staging. Eur Radiol 26:2297–2307
16. Melsaether AN, Raad RA, Pujara AC et al (2016) Comparison of whole-body (18) F FDG PET/MR imaging and whole-body (18) F FDG PET/CT in terms of lesion detection and radiation dose in patients with breast cancer. Radiology 281:193–202
17. Cho IH, Kong EJ (2017) Potential clinical applications of 18F-fluorodeoxyglucose positron emission tomography/magnetic resonance mammography in breast cancer. Nucl Med Mol Imaging 51: 217–226
18. Grueneisen J, Sawicki LM, Wetter A et al (2017) Evaluation of PET and MR datasets in integrated 18F-FDG PET/MRI: A comparison of different MR sequences for whole-body restaging of breast cancer patients. Eur J Radiol 89:14–19
19. Ohno Y, Kauczor HU, Hatabu H, Seo JB, van Beek EJR; International Workshop for Pulmonary Functional Imaging (IWPFI) (2018) MRI for solitary pulmonary nodule and mass assessment: current state of the art. J Magn Reson Imaging 47:1437–1458
20. Sawicki LM, Grueneisen J, Schaarschmidt BM et al (2016) Evaluation of (1)(8)F-FDG PET/MRI, (1)(8)F-FDG PET/CT, MRI, and CT in whole-body staging of recurrent breast cancer. Eur J Radiol 85:459–465
21. Pace L, Nicolai E, Luongo A et al (2014) Comparison of whole-body PET/CT and PET/MRI in breast cancer patients: lesion detection and quantitation of 18F-deoxyglucose uptake in lesions and in normal organ tissues. Eur J Radiol 83:289–296
22. Dregely I, Lanz T, Metz S et al (2015) A 16-channel MR coil for simultaneous PET/MR imaging in breast cancer. Eur Radiol 25: 1154–1161
23. Kong EJ, Chun KA, Bom HS, Lee J, Lee SJ, Cho IH (2014) Initial experience of integrated PET/MR mammography in patients with invasive ductal carcinoma. Hell J Nucl Med 17:171–176
24. Wang J, Shih TT, Yen RF (2017) Multiparametric evaluation of treatment response to neoadjuvant chemotherapy in breast cancer using integrated PET/MR. Clin Nucl Med 42:506–513
25. Wangerin KA, Muzi M, Peterson LM et al (2015) Effect of ^{18}F-FDG uptake time on lesion detectability in PET imaging of early stage breast cancer. Tomography 1:53–60
26. Boerner AR, Weckesser M, Herzog H et al (1999) Optimal scan time for fluorine-18 fluorodeoxyglucose positron emission tomography in breast cancer. Eur J Nucl Med 26:226–230
27. Catalano OA, Daye D, Signore A et al (2017) Staging performance of whole-body DWI, PET/CT and PET/MRI in invasive ductal carcinoma of the breast. Int J Oncol 51:281–288
28. van Nijnatten TJA, Goorts B, Vöö S et al (2018) Added value of dedicated axillary hybrid 18F-FDG PET/MRI for improved axillary nodal staging in clinically node-positive breast cancer patients: a feasibility study. Eur J Nucl Med Mol Imaging 45:179–186